Letter

Search for the decay $D^0 \to \pi^0 \nu \bar{\nu}$

M. Ablikim,[1] M. N. Achasov,[10,b] P. Adlarson,[66] S. Ahmed,[14] M. Albrecht,[4] R. Aliberti,[27] A. Amoroso,[65a,65c] M. R. An,[31] Q. An,[62,48] X. H. Bai,[56] Y. Bai,[47] O. Bakina,[28] R. Baldini Ferroli,[22a] I. Balossino,[23a] Y. Ban,[37,g] K. Begzsuren,[25] N. Berger,[27] M. Bertani,[22a] D. Bettoni,[23a] F. Bianchi,[65a,65c] J. Bloms,[59] A. Bortone,[65a,65c] I. Boyko,[28] R. A. Briere,[5] A. Brueggemann,[59] H. Cai,[67] X. Cai,[1,48] A. Calcaterra,[22a] G. F. Cao,[1,53] N. Cao,[1,53] S. A. Cetin,[52a] J. F. Chang,[1,48] W. L. Chang,[1,53] G. Chelkov,[28,a] G. Chen,[1] H. S. Chen,[1,53] M. L. Chen,[1,48] S. J. Chen,[34] X. R. Chen,[24,53] Y. B. Chen,[1,48] Z. J. Chen,[19,h] W. S. Cheng,[65c] G. Cibinetto,[23a] F. Cossio,[65c] H. L. Dai,[1,48] X. C. Dai,[1,53] A. Dbeyssi,[14] R. E. de Boer,[4] D. Dedovich,[28] Z. Y. Deng,[1] A. Denig,[27] I. Denysenko,[28] M. Destefanis,[65a,65c] F. De Mori,[65a,65c] Y. Ding,[32] J. Dong,[1,48] L. Y. Dong,[1,53] M. Y. Dong,[1,48,53] X. Dong,[67] S. X. Du,[70] Y. L. Fan,[67] J. Fang,[1,48] S. S. Fang,[1,53] Y. Fang,[1] R. Farinelli,[23a] L. Fava,[65b,65c] F. Feldbauer,[4] G. Felici,[22a] C. Q. Feng,[62,48] J. H. Feng,[49] M. Fritsch,[4] C. D. Fu,[1] Y. N. Gao,[37,g] Ya Gao,[63] Yang Gao,[62,48] I. Garzia,[23a,23b] P. T. Ge,[67] C. Geng,[49] E. M. Gersabeck,[57] A. Gilman,[60] K. Goetzen,[11] L. Gong,[32] W. X. Gong,[1,48] W. Gradl,[27] M. Greco,[65a,65c] L. M. Gu,[34] M. H. Gu,[1,48] C. Y. Guan,[1,53] L. B. Guo,[33] R. P. Guo,[39] Y. P. Guo,[9,f] A. Guskov,[28,a] T. T. Han,[40] W. Y. Han,[31] X. Q. Hao,[15] F. A. Harris,[55] K. L. He,[1,53] F. H. Heinsius,[4] C. H. Heinz,[27] Y. K. Heng,[1,48,53] C. Herold,[50] M. Himmelreich,[11,d] T. Holtmann,[4] G. Y. Hou,[1,53] Y. R. Hou,[53] Z. L. Hou,[1] H. M. Hu,[1,53] J. F. Hu,[46,i] T. Hu,[1,48,53] Y. Hu,[1] G. S. Huang,[62,48] L. Q. Huang,[63] X. T. Huang,[40] Y. P. Huang,[1] Z. Huang,[37,g] T. Hussain,[64] N. Hüsken,[21,27] W. Imoehl,[21] M. Irshad,[62,48] J. Jackson,[21] S. Jaeger,[4] S. Janchiv,[25] Q. Ji,[1] Q. P. Ji,[15] X. B. Ji,[1,53] X. L. Ji,[1,48] Y. Y. Ji,[40] H. B. Jiang,[40] X. S. Jiang,[1,48,53] Y. Jiang,[53] J. B. Jiao,[40] Z. Jiao,[17] S. Jin,[34] Y. Jin,[56] M. Q. Jing,[1,53] T. Johansson,[66] N. Kalantar-Nayestanaki,[54] X. S. Kang,[32] R. Kappert,[54] M. Kavatsyuk,[54] B. C. Ke,[70] I. K. Keshk,[4] A. Khoukaz,[59] P. Kiese,[27] R. Kiuchi,[1] R. Kliemt,[11] L. Koch,[29] O. B. Kolcu,[52a] B. Kopf,[4] M. Kuemmel,[4] M. Kuessner,[4] A. Kupsc,[66] M. G. Kurth,[1,53] W. Kühn,[29] J. J. Lane,[57] J. S. Lange,[29] P. Larin,[14] A. Lavania,[20] L. Lavezzi,[65a,65c] Z. H. Lei,[62,48] H. Leithoff,[27] M. Lellmann,[27] T. Lenz,[27] C. Li,[38] C. H. Li,[31] Cheng Li,[62,48] D. M. Li,[70] F. Li,[1,48] G. Li,[1] H. Li,[62,48] H. Li,[42] H. B. Li,[1,53] H. J. Li,[15] J. Q. Li,[4] J. S. Li,[49] J. W. Li,[40] Ke Li,[1] L. K. Li,[1] Lei Li,[3] P. R. Li,[30,j,k] S. Y. Li,[51] W. D. Li,[1,53] W. G. Li,[1] X. H. Li,[62,48] X. L. Li,[40] Xiaoyu Li,[1,53] Z. Y. Li,[49] H. Liang,[62,48] H. Liang,[1,53] H. Liang,[26] Y. F. Liang,[44] Y. T. Liang,[24,53] G. R. Liao,[12] L. Z. Liao,[1,53] L. Z. Liao,[40] J. Libby,[20] A. Limphirat,[50] C. X. Lin,[49] T. Lin,[1] B. J. Liu,[1] C. X. Liu,[1] D. Liu,[14,62] F. H. Liu,[43] Fang Liu,[1] Feng Liu,[6] H. M. Liu,[1,53] Huanhuan Liu,[1] Huihui Liu,[16] J. B. Liu,[62,48] J. L. Liu,[63] J. Y. Liu,[1,53] K. Liu,[1] K. Y. Liu,[32] L. Liu,[62,48] M. H. Liu,[9,f] P. L. Liu,[1] Q. Liu,[67] Q. Liu,[53] S. B. Liu,[62,48] Shuai Liu,[45] T. Liu,[1,53] W. M. Liu,[62,48] X. Liu,[30,j,k] Y. Liu,[30,j,k] Y. B. Liu,[35] Z. A. Liu,[1,48,53] Z. Q. Liu,[40] X. C. Lou,[1,48,53] F. X. Lu,[49] H. J. Lu,[17] J. D. Lu,[1,53] J. G. Lu,[1,48] X. L. Lu,[1] Y. Lu,[1] Y. P. Lu,[1,48] C. L. Luo,[33] M. X. Luo,[69] T. Luo,[9,f] X. L. Luo,[1,48] X. R. Lyu,[53] F. C. Ma,[32] H. L. Ma,[1] L. L. Ma,[40] M. M. Ma,[1,53] Q. M. Ma,[1] R. Q. Ma,[1,53] R. T. Ma,[53] X. X. Ma,[1,53] X. Y. Ma,[1,48] Y. Ma,[37,g] F. E. Maas,[14] M. Maggiora,[65a,65c] S. Maldaner,[4] S. Malde,[60] Q. A. Malik,[64] A. Mangoni,[22b] Y. J. Mao,[37,g] Z. P. Mao,[1] S. Marcello,[65a,65c] Z. X. Meng,[56] J. G. Messchendorp,[54,11] G. Mezzadri,[23a] T. J. Min,[34] R. E. Mitchell,[21] X. H. Mo,[1,48,53] N. Yu. Muchnoi,[10,b] H. Muramatsu,[58] S. Nakhoul,[11,d] Y. Nefedov,[28] F. Nerling,[11,d] I. B. Nikolaev,[10,b] Z. Ning,[1,48] S. Nisar,[8,l] S. L. Olsen,[53] Q. Ouyang,[1,48,53] S. Pacetti,[22b,22c] X. Pan,[9,f] Y. Pan,[57] A. Pathak,[1] A. Pathak,[26] P. Patteri,[22a] M. Pelizaeus,[4] H. P. Peng,[62,48] K. Peters,[11,d] J. Pettersson,[66] J. L. Ping,[33] R. G. Ping,[1,53] S. Pogodin,[28] R. Poling,[58] V. Prasad,[62,48] H. Qi,[62,48] H. R. Qi,[51] K. H. Qi,[24] M. Qi,[34] T. Y. Qi,[9,f] S. Qian,[1,48] W. B. Qian,[53] Z. Qian,[49] C. F. Qiao,[53] L. Q. Qin,[12] X. P. Qin,[9,f] X. S. Qin,[40] Z. H. Qin,[1,48] J. F. Qiu,[1] S. Q. Qu,[35] S. Q. Qu,[51] K. H. Rashid,[64] K. Ravindran,[20] C. F. Redmer,[27] A. Rivetti,[65c] V. Rodin,[54] M. Rolo,[65c] G. Rong,[1,53] Ch. Rosner,[14] M. Rump,[59] H. S. Sang,[62] A. Sarantsev,[28,c] Y. Schelhaas,[27] C. Schnier,[4] K. Schoenning,[66] M. Scodeggio,[23a,23b] D. C. Shan,[45] W. Shan,[18] X. Y. Shan,[62,48] J. F. Shangguan,[45] M. Shao,[62,48] C. P. Shen,[9,f] H. F. Shen,[1,53] P. X. Shen,[35] X. Y. Shen,[1,53] H. C. Shi,[62,48] R. S. Shi,[1,53] X. Shi,[1,48] X. D. Shi,[62,48] W. M. Song,[26,1] Y. X. Song,[37,g] S. Sosio,[65a,65c] S. Spataro,[65a,65c] K. X. Su,[67] P. P. Su,[45] G. X. Sun,[1] H. K. Sun,[1] J. F. Sun,[15] L. Sun,[67] S. S. Sun,[1,53] T. Sun,[1,53] W. Y. Sun,[26] W. Y. Sun,[33] X. Sun,[19,h] Y. J. Sun,[62,48] Y. Z. Sun,[1] Z. T. Sun,[40] Y. H. Tan,[67] Y. X. Tan,[62,48] C. J. Tang,[44] G. Y. Tang,[1] J. Tang,[49] J. X. Teng,[62,48] V. Thoren,[66] W. H. Tian,[42] Y. Tian,[24,53] I. Uman,[52b] B. Wang,[1] B. L. Wang,[53] C. W. Wang,[34] D. Y. Wang,[37,g] H. J. Wang,[30,j,k] H. P. Wang,[1,53] K. Wang,[1,48] L. L. Wang,[1] M. Wang,[40] M. Z. Wang,[37,g] Meng Wang,[1,53] S. Wang,[9,f] W. Wang,[49] W. H. Wang,[67] W. P. Wang,[62,48] X. Wang,[37,g] X. F. Wang,[30,j,k] X. L. Wang,[9,f] Y. Wang,[62,48] Y. D. Wang,[36] Y. F. Wang,[1,48,53] Y. Q. Wang,[1] Ying Wang,[49] Z. Wang,[1,48] Z. Y. Wang,[1,53] Ziyi Wang,[53] Zongyuan Wang,[1,53] D. H. Wei,[12] F. Weidner,[59] S. P. Wen,[1] D. J. White,[57] U. Wiedner,[4] G. Wilkinson,[60] M. Wolke,[66] L. Wollenberg,[4] J. F. Wu,[1,53] L. H. Wu,[1] L. J. Wu,[1,53] X. Wu,[9,f] Z. Wu,[1,48] L. Xia,[62,48] T. Xiang,[37,g] H. Xiao,[9,f] S. Y. Xiao,[1] Z. J. Xiao,[33] X. H. Xie,[37,g] Y. Xie,[40] Y. G. Xie,[1,48] Y. H. Xie,[6] Z. P. Xie,[62,48] T. Y. Xing,[1,53] C. J. Xu,[49] G. F. Xu,[1] Q. J. Xu,[13] S. Y. Xu,[61] W. Xu,[1,53] X. P. Xu,[45] Y. C. Xu,[53] F. Yan,[9,f] L. Yan,[9,f] W. B. Yan,[62,48] W. C. Yan,[70] Xu Yan,[45] H. J. Yang,[41,e] H. X. Yang,[1] L. Yang,[42] S. L. Yang,[53] Yifan Yang,[1,53] Zhi Yang,[24] M. Ye,[1,48] M. H. Ye,[7] J. H. Yin,[1] Z. Y. You,[49] B. X. Yu,[1,48,53] C. X. Yu,[35] G. Yu,[1,53] J. S. Yu,[19,h] T. Yu,[63] C. Z. Yuan,[1,53] L. Yuan,[2] X. Q. Yuan,[37,g] Y. Yuan,[1,53] Z. Y. Yuan,[49] C. X. Yue,[31] A. A. Zafar,[64] X. Zeng Zeng,[6] Y. Zeng,[19,h] A. Q. Zhang,[1] B. X. Zhang,[1] G. Y. Zhang,[15] H. Zhang,[62]

H. H. Zhang,[49] H. H. Zhang,[26] H. Y. Zhang,[1,48] J. L. Zhang,[68] J. Q. Zhang,[33] J. W. Zhang,[1,48,53] J. Y. Zhang,[1] J. Z. Zhang,[1,53] Jianyu Zhang,[1,53] Jiawei Zhang,[1,53] L. M. Zhang,[51] L. Q. Zhang,[49] Lei Zhang,[34] S. F. Zhang,[34] Shulei Zhang,[19,h] X. D. Zhang,[36] X. Y. Zhang,[40] Y. Zhang,[60] Y. T. Zhang,[70] Y. H. Zhang,[1,48] Yan Zhang,[62,48] Yao Zhang,[1] Z. Y. Zhang,[67] G. Zhao,[1] J. Zhao,[31] J. Y. Zhao,[1,53] J. Z. Zhao,[1,48] Lei Zhao,[62,48] Ling Zhao,[1] M. G. Zhao,[35] Q. Zhao,[1] S. J. Zhao,[70] Y. B. Zhao,[1,48] Y. X. Zhao,[24,53] Z. G. Zhao,[62,48] A. Zhemchugov,[28,a] B. Zheng,[63] J. P. Zheng,[1,48] Y. H. Zheng,[53] B. Zhong,[33] C. Zhong,[63] H. Zhou,[40] L. P. Zhou,[1,53] Q. Zhou,[1,53] X. Zhou,[67] X. K. Zhou,[53] X. R. Zhou,[62,48] X. Y. Zhou,[31] A. N. Zhu,[1,53] J. Zhu,[35] K. Zhu,[1] K. J. Zhu,[1,48,53] S. H. Zhu,[61] T. J. Zhu,[68] W. J. Zhu,[9,f] W. J. Zhu,[35] Y. C. Zhu,[62,48] Z. A. Zhu,[1,53] B. S. Zou,[1] and J. H. Zou[1]

(BESIII Collaboration)

[1]*Institute of High Energy Physics, Beijing 100049, People's Republic of China*
[2]*Beihang University, Beijing 100191, People's Republic of China*
[3]*Beijing Institute of Petrochemical Technology, Beijing 102617, People's Republic of China*
[4]*Bochum Ruhr-University, D-44780 Bochum, Germany*
[5]*Carnegie Mellon University, Pittsburgh, Pennsylvania 15213, USA*
[6]*Central China Normal University, Wuhan 430079, People's Republic of China*
[7]*China Center of Advanced Science and Technology, Beijing 100190, People's Republic of China*
[8]*COMSATS University Islamabad, Lahore Campus, Defence Road, Off Raiwind Road, 54000 Lahore, Pakistan*
[9]*Fudan University, Shanghai 200433, People's Republic of China*
[10]*G.I. Budker Institute of Nuclear Physics SB RAS (BINP), Novosibirsk 630090, Russia*
[11]*GSI Helmholtzcentre for Heavy Ion Research GmbH, D-64291 Darmstadt, Germany*
[12]*Guangxi Normal University, Guilin 541004, People's Republic of China*
[13]*Hangzhou Normal University, Hangzhou 310036, People's Republic of China*
[14]*Helmholtz Institute Mainz, Staudinger Weg 18, D-55099 Mainz, Germany*
[15]*Henan Normal University, Xinxiang 453007, People's Republic of China*
[16]*Henan University of Science and Technology, Luoyang 471003, People's Republic of China*
[17]*Huangshan College, Huangshan 245000, People's Republic of China*
[18]*Hunan Normal University, Changsha 410081, People's Republic of China*
[19]*Hunan University, Changsha 410082, People's Republic of China*
[20]*Indian Institute of Technology Madras, Chennai 600036, India*
[21]*Indiana University, Bloomington, Indiana 47405, USA*
[22a]*INFN Laboratori Nazionali di Frascati, INFN Laboratori Nazionali di Frascati I-00044, Frascati, Italy*
[22b]*INFN Laboratori Nazionali di Frascati, INFN Sezione di Perugia, I-06100, Perugia, Italy*
[22c]*INFN Laboratori Nazionali di Frascati, University of Perugia, I-06100, Perugia, Italy*
[23a]*INFN Sezione di Ferrara, INFN Sezione di Ferrara, I-44122, Ferrara, Italy*
[23b]*INFN Sezione di Ferrara, University of Ferrara, I-44122, Ferrara, Italy*
[24]*Institute of Modern Physics, Lanzhou 730000, People's Republic of China*
[25]*Institute of Physics and Technology, Peace Ave. 54B, Ulaanbaatar 13330, Mongolia*
[26]*Jilin University, Changchun 130012, People's Republic of China*
[27]*Johannes Gutenberg University of Mainz, Johann-Joachim-Becher-Weg 45, D-55099 Mainz, Germany*
[28]*Joint Institute for Nuclear Research, 141980 Dubna, Moscow, Russia*
[29]*Justus-Liebig-Universitaet Giessen, II. Physikalisches Institut, Heinrich-Buff-Ring 16, D-35392 Giessen, Germany*
[30]*Lanzhou University, Lanzhou 730000, People's Republic of China*
[31]*Liaoning Normal University, Dalian 116029, People's Republic of China*
[32]*Liaoning University, Shenyang 110036, People's Republic of China*
[33]*Nanjing Normal University, Nanjing 210023, People's Republic of China*
[34]*Nanjing University, Nanjing 210093, People's Republic of China*
[35]*Nankai University, Tianjin 300071, People's Republic of China*
[36]*North China Electric Power University, Beijing 102206, People's Republic of China*
[37]*Peking University, Beijing 100871, People's Republic of China*
[38]*Qufu Normal University, Qufu 273165, People's Republic of China*
[39]*Shandong Normal University, Jinan 250014, People's Republic of China*
[40]*Shandong University, Jinan 250100, People's Republic of China*
[41]*Shanghai Jiao Tong University, Shanghai 200240, People's Republic of China*
[42]*Shanxi Normal University, Linfen 041004, People's Republic of China*

[43]*Shanxi University, Taiyuan 030006, People's Republic of China*
[44]*Sichuan University, Chengdu 610064, People's Republic of China*
[45]*Soochow University, Suzhou 215006, People's Republic of China*
[46]*South China Normal University, Guangzhou 510006, People's Republic of China*
[47]*Southeast University, Nanjing 211100, People's Republic of China*
[48]*State Key Laboratory of Particle Detection and Electronics, Beijing 100049, Hefei 230026, People's Republic of China*
[49]*Sun Yat-Sen University, Guangzhou 510275, People's Republic of China*
[50]*Suranaree University of Technology, University Avenue 111, Nakhon Ratchasima 30000, Thailand*
[51]*Tsinghua University, Beijing 100084, People's Republic of China*
[52a]*Turkish Accelerator Center Particle Factory Group, Istinye University, 34010, Istanbul, Turkey*
[52b]*Turkish Accelerator Center Particle Factory Group, Near East University, Nicosia, North Cyprus, Mersin 10, Turkey*
[53]*University of Chinese Academy of Sciences, Beijing 100049, People's Republic of China*
[54]*University of Groningen, NL-9747 AA Groningen, The Netherlands*
[55]*University of Hawaii, Honolulu, Hawaii 96822, USA*
[56]*University of Jinan, Jinan 250022, People's Republic of China*
[57]*University of Manchester, Oxford Road, Manchester, M13 9PL, United Kingdom*
[58]*University of Minnesota, Minneapolis, Minnesota 55455, USA*
[59]*University of Muenster, Wilhelm-Klemm-Str. 9, 48149 Muenster, Germany*
[60]*University of Oxford, Keble Rd, Oxford OX1 3RH, United Kingdom*
[61]*University of Science and Technology Liaoning, Anshan 114051, People's Republic of China*
[62]*University of Science and Technology of China, Hefei 230026, People's Republic of China*
[63]*University of South China, Hengyang 421001, People's Republic of China*
[64]*University of the Punjab, Lahore-54590, Pakistan*
[65a]*University of Turin and INFN, University of Turin, I-10125 Turin, Italy*
[65b]*University of Turin and INFN, University of Eastern Piedmont, I-15121, Alessandria, Italy*
[65c]*University of Turin and INFN, INFN, I-10125 Turin, Italy*
[66]*Uppsala University, Box 516, SE-75120 Uppsala, Sweden*
[67]*Wuhan University, Wuhan 430072, People's Republic of China*
[68]*Xinyang Normal University, Xinyang 464000, People's Republic of China*
[69]*Zhejiang University, Hangzhou 310027, People's Republic of China*
[70]*Zhengzhou University, Zhengzhou 450001, People's Republic of China*

(Received 31 December 2021; accepted 4 April 2022; published 21 April 2022)

We present the first experimental search for the rare charm decay $D^0 \to \pi^0 \nu\bar{\nu}$. It is based on an e^+e^- collision sample consisting of 10.6×10^6 pairs of $D^0\bar{D}^0$ mesons collected by the BESIII detector at $\sqrt{s} = 3.773$ GeV, corresponding to an integrated luminosity of 2.93 fb^{-1}. A data-driven method is used to ensure the reliability of the background modeling. No significant $D^0 \to \pi^0 \nu\bar{\nu}$ signal is observed in data and

[a]Also at the Moscow Institute of Physics and Technology, Moscow 141700, Russia.
[b]Also at the Novosibirsk State University, Novosibirsk 630090, Russia.
[c]Also at the NRC "Kurchatov Institute", PNPI, 188300 Gatchina, Russia.
[d]Also at Goethe University Frankfurt, 60323 Frankfurt am Main, Germany.
[e]Also at Key Laboratory for Particle Physics, Astrophysics and Cosmology, Ministry of Education; Shanghai Key Laboratory for Particle Physics and Cosmology; Institute of Nuclear and Particle Physics, Shanghai 200240, People's Republic of China.
[f]Also at Key Laboratory of Nuclear Physics and Ion-beam Application (MOE) and Institute of Modern Physics, Fudan University, Shanghai 200443, People's Republic of China.
[g]Also at State Key Laboratory of Nuclear Physics and Technology, Peking University, Beijing 100871, People's Republic of China.
[h]Also at School of Physics and Electronics, Hunan University, Changsha 410082, China.
[i]Also at Guangdong Provincial Key Laboratory of Nuclear Science, Institute of Quantum Matter, South China Normal University, Guangzhou 510006, China.
[j]Also at Frontiers Science Center for Rare Isotopes, Lanzhou University, Lanzhou 730000, People's Republic of China.
[k]Also at Lanzhou Center for Theoretical Physics, Lanzhou University, Lanzhou 730000, People's Republic of China.
[l]Also at the Department of Mathematical Sciences, IBA, Karachi, Pakistan.

an upper limit of the branching fraction is set to be 2.1×10^{-4} at the 90% confidence level. This is the first experimental constraint on charmed-hadron decays into dineutrino final states.

DOI: 10.1103/PhysRevD.105.L071102

Flavor changing neutral current (FCNC) transitions in the Standard Model (SM) are highly suppressed by the Glashow-Iliopoulos-Maiani(GIM) mechanism [1]. GIM suppression is more effective for the charm sector compared to the down-type quarks in the bottom and strange sectors. This suppression is responsible for the relatively small size of charm mixing and CP violation in the charm system [2–4]. Therefore, FCNC processes involving D decays into charged lepton pairs are often totally overshadowed by long distance contributions [5,6]. However, for D FCNC decays into final states involving dineutrinos, such as $D^0 \to \pi^0 \nu\bar{\nu}$, long-distance contributions become insignificant and the short-distance contributions from Z-penguin and box diagrams dominate, resulting in the branching fraction at the level of 10^{-15} in SM [7]. That makes D FCNC decay involving dineutrinos a unique and clean probe to study the CP violation in the charm sector [8] and search for new physics beyond SM [9]. Such new physics effects can enhance the branching fraction largely above the tiny values in SM [10,11].

Recently, LHCb reported evidence for the breaking of lepton universality in bottom-quark FCNC decays to charged dielectrons and dimuons with a significance of 3.1σ [12], which suggests the possible presence of new physics contributions in the lepton sector [13]. For instance, a popular proposal of leptoquarks beyond SM, which have different interaction strengths with the different types of leptons, can naturally accommodate the lepton universality breaking [10,14]. A complementary study on the FCNC decay $D^0 \to \pi^0 \nu\bar{\nu}$ is necessary to test the flavor structure of leptons given its extremely suppressed decay rate [7] in SM. In the scenario of leptoquarks, the branching fraction can be enhanced up to 9.7×10^{-4} with inclusion of the sterile neutrinos [15].

Charm decays with a neutrino pair in the final state have never been searched for experimentally. Taking advantage of the clean environment of threshold production, the first search for D meson FCNC decays involving dineutrinos is performed based on the 2.93 fb^{-1} e^+e^- annihilation data sample collected at $\sqrt{s} = 3.773$ GeV by the BESIII detector [16]. This sample consists of 10.6×10^6 pairs of $D^0\bar{D}^0$ mesons and 8.3×10^6 pairs of D^+D^- mesons [17]. Decays of D^0 mesons into dineutrino final states are more suitable for study than those of their charged counterpart, as D^+ decays of this nature suffer from irreducible contamination from the process $D^+ \to \tau^+\nu_\tau$, where the τ lepton decays into mesons and a neutrino. Consequently, this letter reports a search for the FCNC decay $D^0 \to \pi^0 \nu\bar{\nu}$. For this decay process, a reliable modeling of the background contributions is crucial. This requirement is best achieved through a sophisticated data-driven method. About one third of the full data sample is used to validate the data-driven analysis procedure, and the final results are obtained by unblinding the total data set after the analysis strategy is fixed.

Details about the BESIII detector design and performance are given in Ref. [18]. A generic Monte Carlo (MC) simulated data sample, described in Ref. [19], is employed to identify sources of background contributions. The signal process $D^0 \to \pi^0 \nu\bar{\nu}$ is simulated following the model described in Ref. [10], incorporating associated $D \to \pi$ form factors in the form of a single-pole model with parameters measured in Ref. [20].

Since the center-of-mass energy of 3.773 GeV is just above the $D\bar{D}$ mass threshold, the D^0 and $\bar{D}^0$ mesons are produced almost at rest without any additional hadrons in the event. Hence, it is straightforward to use a double-tag approach [21,22] to measure the absolute branching fraction of $D^0 \to \pi^0 \nu\bar{\nu}$, $\mathcal{B}_{\rm sig}$, according to

$$\mathcal{B}_{\rm sig} = \frac{N_{\rm sig}}{\mathcal{B}_{\pi^0\to\gamma\gamma} \sum_\alpha N^\alpha_{\rm tag} \epsilon^\alpha_{\rm tag,sig} / \epsilon^\alpha_{\rm tag}}. \quad (1)$$

Here, α represents the different single-tag modes, $N^\alpha_{\rm tag}$ is the single-tag yield for tag mode α, $N_{\rm sig}$ is the sum of the double-tag yields from all single-tag modes, $\epsilon^\alpha_{\rm tag}$ and $\epsilon^\alpha_{\rm tag,sig}$ refer to the corresponding single-tag efficiency and the double-tag efficiency, respectively, for the tag-mode α as determined by MC simulations, and $\mathcal{B}_{\pi^0\to\gamma\gamma}$ is the branching fraction of $\pi^0 \to \gamma\gamma$. In this approach, the systematic uncertainties arising from the single-tag reconstruction are canceled out. Throughout this paper, charge-conjugate modes are always implied.

A detailed description of the selection criteria for charged and neutral particle candidates is provided in Ref. [19]. The single-tag $\bar{D}^0$ candidates are reconstructed by appropriate combinations of the charged tracks and π^0 candidates forming the three hadronic channels: $K^+\pi^-$, $K^+\pi^-\pi^0$ and $K^+\pi^-\pi^+\pi^-$. The candidates are selected using two variables calculated in the e^+e^- center-of-mass frame; the beam-constrained mass $M_{\rm BC} = \sqrt{E^2_{\rm beam}/c^4 - |\mathbf{p}_{\bar{D}^0}|^2/c^2}$ and the energy difference $\Delta E = E_{\bar{D}^0} - E_{\rm beam}$. Here, $E_{\rm beam}$ is the energy of the electron beam and $E_{\bar{D}^0}$ and $\mathbf{p}_{\bar{D}^0}$ are the total energy and momentum, respectively, of all final-state particles of the $\bar{D}^0$ candidate. If there are multiple combinations for each tag mode in one event, the candidate with

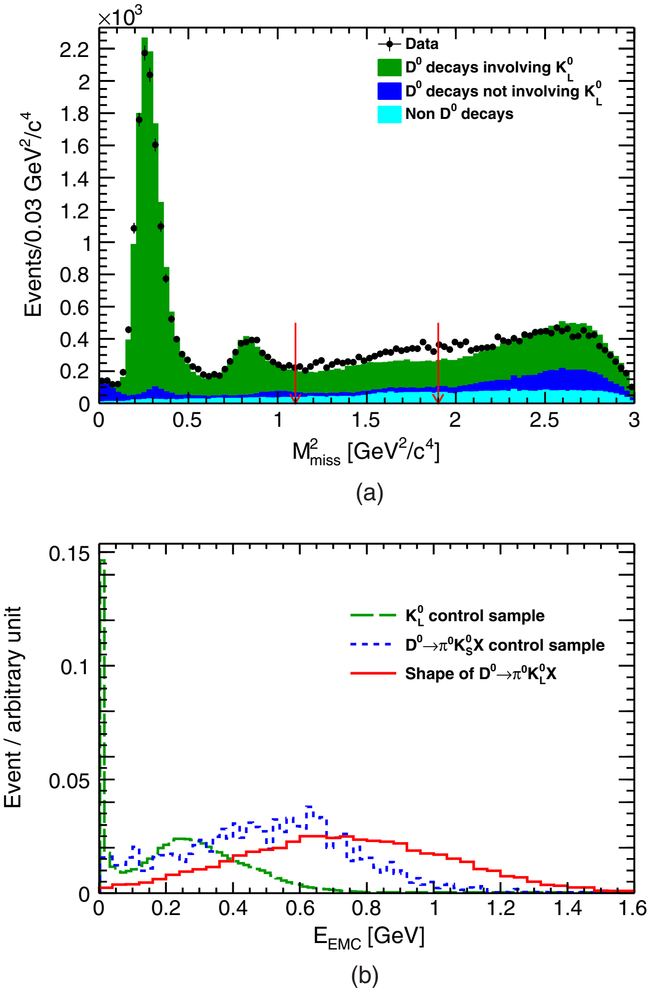

FIG. 1. (a) $M^2_{\rm miss}$ distribution in data and generic MC sample. The black dots with uncertainties represent data and the filled areas show the background components estimated from generic MC sample. The green, blue, and cerulean filled areas represent the background components of D^0 decays with a K^0_L meson in the final state, D^0 decays without K^0_L meson in the final state and non-D^0 decays, respectively. The vertical arrows indicate the selected region. (b) Distributions of $E_{\rm EMC}$, the summed calorimeter energy unassociated with signal and tag decays. The red solid line shows the distribution of the $D^0 \to \pi^0 K^0_L X$ background. Energy deposit of K^0_L and X obtained from the corresponding control samples are marked as green long-dashed and blue dashed lines, respectively. All the distributions are normalized to unity.

the smallest $|\Delta E|$ is chosen. The single-tag yield $N^\alpha_{\rm tag}$ of each tag mode is obtained from a fit to the $M_{\rm BC}$ distribution in data and the efficiency $\epsilon^\alpha_{\rm tag}$ is determined from the generic MC sample following the method in Ref. [19].

After a single-tag $\bar{D}^0$ meson is identified, we reconstruct the signal D^0 decay recoiling against the single-tag $\bar{D}^0$ meson. As the signal final-state particles are all neutral, we require there are no charged tracks in addition to those of the tagged $\bar{D}^0$ meson. Furthermore, it is required that only one π^0 candidate can be formed from any pairs of photon candidates not used to reconstruct the tagged $\bar{D}^0$ meson. The invariant mass of two photons for the π^0 candidate must satisfy $M_{\gamma\gamma} \in (0.115, 0.150)$ GeV$/c^2$ and pass the kinematic fit constraining $M_{\gamma\gamma}$ to the nominal π^0 mass. The χ^2 of the kinematic fit is required to be less than 20 to improve background suppression. By studying the generic MC sample [23], we find the surviving backgrounds mainly come from D^0 decays involving a K^0_L meson. Figure 1(a) presents the distribution of the recoil mass $M^2_{\rm miss}c^2 = (p_{e^+e^-} - p_{\bar{D}^0} - p_{\pi^0})^2$, where the four-momenta $p_{e^+e^-}$, $p_{\bar{D}^0}$, and p_{π^0} of the initial e^+e^- system, the tag $\bar{D}^0$, and the signal-side π^0, respectively, are evaluated in the e^+e^- center-of-mass system. Two peaks around 0.25 GeV$^2/c^4$ and 0.80 GeV$^2/c^4$ are prominent, which correspond to the processes $D^0 \to K^0_L \pi^0$ and $\bar{K}^*(892)^0\pi^0$, respectively. To remove these background contributions, only events with $M^2_{\rm miss} \in (1.1, 1.9)$ GeV$^2/c^4$ are retained. The upper bound is applied to suppress the backgrounds with multiple charged and neutral soft pions, which give rise to a broad bump near the kinematic limit of 3.0 GeV$^2/c^4$. After imposing all the above requirements on the signal MC samples, the ratios of $\epsilon^\alpha_{\rm tag,sig}/\epsilon^\alpha_{\rm tag}$ in Eq. (1) are determined to be $(14.90 \pm 0.11)\%$, $(13.04 \pm 0.15)\%$ and $(11.76 \pm 0.13)\%$ for the three tag modes of $K^+\pi^-$, $K^+\pi^-\pi^0$, and $K^+\pi^-\pi^+\pi^-$, respectively. In the subsequent analysis the summed energy $E_{\rm EMC}$ of all the showers deposited in the electromagnetic calorimeter, excluding those used to reconstruct the π^0's from the singly-tagged and signal D decays is fitted as a discriminating variable. Signals are expected to peak close to zero.

The residual background surviving the selection is found to be dominated by $D^0 \to \pi^0 K^0_L X$ decays, where X denotes multiple neutral and charged soft pions. The energy deposit of these events is not well described in the generic MC sample as is evident from the discrepancy between data and MC in Fig. 1(a). This discrepancy is attributed both to the poorly known branching fractions of these decays, and the imperfect simulation of the interaction between K^0_L mesons and the detector material by Geant4 [24]. Therefore, the energy deposits of K^0_L and X are modeled in a data-driven method with control samples as discussed below.

The energy deposit of K^0_L mesons is studied with a control sample selected from a data set of $1,087 \times 10^6$ J/ψ decays [25]. Two control samples of $J/\psi \to \phi K^\pm \pi^\mp K^0_L$ and $J/\psi \to K^\pm \pi^\mp K^0_L$ are selected with a signal purity of about 99%. The K^0_L-induced showers within 10° with respect to the K^0_L flight direction are counted. The 10° cone requirement helps to suppress the contamination from beam background and bremsstrahlung radiation from charged tracks. According to MC simulations, the unaccounted showers outside the 10° cone are generally less than 50 MeV and on average 75% of the energy deposited by the K^0_L can be reconstructed within the cone. In order to recover the showers that are unaccounted for, we correct the obtained energy deposit in the control sample with a multidimensional reweighting method as described in Ref. [26], according to a correction factor predicted from single-track K_L^0 simulations as a function of the K_L^0 momentum $P_{K_L^0}$, the cosine of the polar angle $\cos\theta_{K_L^0}$ and the energy deposit $E_{\rm EMC}^{K_L^0}$.

The energy deposit arising from X in the $D^0 \to \pi^0 K_L^0 X$ decays is studied in a control sample of $D^0 \to \pi^0 K_S^0 X$, $K_S^0 \to \pi^+\pi^-$ events. In the $\bar{D}^0$ single-tagged events, we require additional π^0 and K_S^0 candidates following the selection criteria in Ref. [19] to select the control sample. For the sample size under consideration, the X components are expected to be same in D^0 decays to $\pi^0 K_L^0 X$ and $\pi^0 K_S^0 X$. The purity of the control sample is improved after subtracting non-$D^0\bar{D}^0$ decay contributions according to the $M_{\rm BC}$ sideband events in $\bar{D}^0$ single-tag final states. Those showers that are not associated with $\bar{D}^0$ single-tag tracks, π^0 or K_S^0 decays are summed up to represent the X energy deposit denoted as $E_{\rm EMC}^X$.

To obtain a $E_{\rm EMC}$ distribution that is representative of the $D^0 \to \pi^0 K_L^0 X$ background, we obtain a value for both $E_{\rm EMC}^{K_L^0}$ and $E_{\rm EMC}^X$ by randomly sampling from the two separate control samples and sum them up. In order to account for differences in the momentum distribution of the K_L^0 between the control samples and the decay $D^0 \to \pi^0 K_L^0 X$, the control samples are reweighted to match the K_L^0 momentum distribution in the signal simulation. The signal simulation itself is in turn corrected to account for differences between data and simulation observed in the K_S^0 momentum distribution in $D^0 \to \pi^0 K_S^0 X$.

The sampling variable is dependent on the kinematic variables of the K_L^0 momenta based on MC simulation samples, which are corrected according to the K_S^0 momentum difference observed in the $\pi^0 K_S^0 X$ control sample and simulations. The resulting $E_{\rm EMC}$ distribution for $D^0 \to \pi^0 K_L^0 X$ is shown in Fig. 1(b).

There are two remaining sources of background. One arises from wrongly tagged events from non-$D^0\bar{D}^0$ processes. Their contributions can be estimated with the events in the singly-tagged $M_{\rm BC}$ sideband region, which is defined as $(1.830, 1.855)\,{\rm GeV}/c^2$. The number of the events in the sideband region is 3134 and the corresponding scaling factor of the background numbers in the signal region, which is defined as $(1.858, 1.874)$ GeV$/c^2$, and sideband region is found to be 0.611 ± 0.001 [19], which results in an estimate of 1919 ± 34 background events in data. The other source of contamination is from events with a correct $\bar{D}^0$-tag candidate but without a K_L^0 meson in the D^0 decay final states. These D^0 decay backgrounds involve decay products with soft kaons and pions, which fail to be reconstructed in the detector. This contribution is modeled with a simulated sample of $\psi(3770) \to D^0\bar{D}^0$ decays.

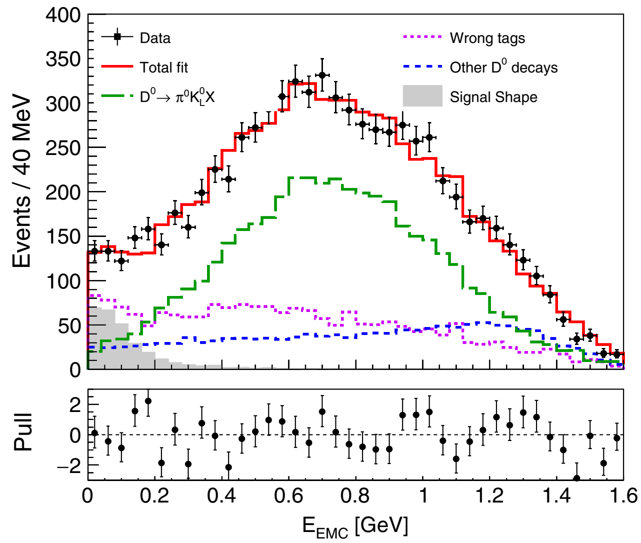

FIG. 2. Fit to the $E_{\rm EMC}$ distribution in data. The black dots with uncertainties represent data and the red solid line shows the total fit. The background components of $D^0 \to K_L^0 \pi^0 X$ decays, wrong $\bar{D}^0$ tags and other D^0 decays are marked as green long-dashed line, purple dotted line, and blue dashed line, respectively. The gray filled area shows the signal shape, normalized to 20 times the central value of the fit result for visibility. The bottom panel shows the fit residuals.

Figure 2 presents the $E_{\rm EMC}$ distribution in data, on which the result of an extended maximum likelihood fit is overlaid. In the fit, the shape of the signal process is modeled according to MC simulations. The yields of all components are free parameters, except for the number of wrongly-tagged $\bar{D}^0$ events, which is fixed to 1919. The fit determines the signal yield $N_{\rm sig}$ to be 14 ± 30, which is consistent with zero. The reduced χ^2 of the goodness-of-fit test is 1.4. As no signal is observed, an upper limit on the branching fraction of $D^0 \to \pi^0 \nu\bar{\nu}$ is estimated after taking into account the systematic uncertainties.

The systematic uncertainties associated with the π^0 reconstruction, the requirement on the number of charged tracks and π^0 candidates, and the requirement on $M_{\rm miss}^2$ are studied with a control sample of $D^0 \to K^-\pi^+\pi^0$ events tagged by the same three $\bar{D}^0$ modes used in this analysis. When imposing our selection requirements, the efficiency differences between data and MC simulations are found to be 2.0%, 4.0%, 1.6%, and 0.7% for the four criteria, respectively. We test the signal model by replacing the $D \to \pi$ form factor with a phase-space model. The resulting efficiency change is found to be 0.5%, which is assigned as the corresponding systematic uncertainty. To investigate possible bias in the estimate of the signal yield from the $D^0 \to \pi^0 K_L^0 X$ modeling, we vary the cone angle to 15° to obtain the K_L^0 energy deposit and repeat the whole analysis procedure. The change in the signal yield is found to be negligible. To determine the size of the uncertainty coming

TABLE I. Summary of systematic uncertainties on the signal yield and detection efficiencies.

Source	Size
Number of π^0	4.0%
π^0 reconstruction	2.0%
Number of charged tracks	1.6%
$M^2_{\rm miss}$ requirement	0.7%
Signal model	0.5%
Wrong-tag background	1.7
$\pi^0 K^0_L X$ background shape	Negligible
Branching fraction of $\pi^0 \to \gamma\gamma$	Negligible

from a wrong estimate of the number of $\bar{D}^0$ wrong-tag events we free this contribution in the fit, with a Gaussian constraint on its uncertainty and find a change on the signal yield of 1.7 compared to the nominal value. The uncertainty of the branching fraction of $\pi^0 \to \gamma\gamma$ is small enough to be neglected [27]. All the systematic uncertainties are summarized in Table I.

To set the upper limit of the branching fraction in Eq. (1) incorporating the systematic uncertainties, we follow the method described in Refs. [28,29]. An ensemble of 100,000 toy samples is generated as a function of $E_{\rm EMC}$ according to the observed data distribution as shown in Fig. 2. In each toy sample, the sample size is randomly sampled from a Poisson distribution with the number of observed events of 7652 in data. A similar fit to the toy sample is carried out as in data, where different systematic uncertainties are randomly varied. The contribution of wrong-$\bar{D}^0$-tag backgrounds is fixed to a value constrained by a Gaussian distribution with the central value of 1919 and uncertainty of 34; the involved values in the denominator in Eq. (1) are randomly assigned according to Gaussian distributions with the nominal values as a mean and their uncertainties corresponding to the standard deviation. The uncertainties associated with the signal-detection efficiencies of the different sources given in Table I, i.e., number of π^0, π^0 reconstruction, number of charged tracks, $M^2_{\rm miss}$ requirement and signal model, are summed up in quadrature. The distribution of the obtained branching fractions in these toy samples is shown in Fig. 3, which follows a Gaussian function as expected. Integrating the Gaussian function in the physical region greater than zero, the upper limit of $\mathcal{B}_{\rm sig}$ is determined to be 2.1×10^{-4} at the 90% confidence level.

In conclusion, we present the first experimental search for the FCNC process $c \to u\nu\bar{\nu}$ through $D^0 \to \pi^0\nu\bar{\nu}$ with 10.6×10^6 pairs of $D^0\bar{D}^0$ mesons produced by e^+e^- collisions near threshold in the BESIII experiment. Adopting the double tag method and data-driven background modeling, no obvious signal is observed and an upper limit on its decay branching fraction is set to be 2.1×10^{-4} at 90% confidence level. This is the world-first experimental constraint in charmed hadron decays to a dineutrino final state. In the absence of sizable long-distance QCD contributions in this process, the result serves as a clean test for CP violation in the charm sector, new physics models beyond SM in FCNC decays, as well as for lepton (flavor) universality. Our result is lower than the upper limit predicted in Ref. [15], hence, providing constrains on the fermionic coupling strength of leptoquarks to the sterile neutrinos. In the future, more stringent results will be available based on an anticipated larger $\psi(3770)$ data set of about 20 fb^{-1} at BESIII [22,30].

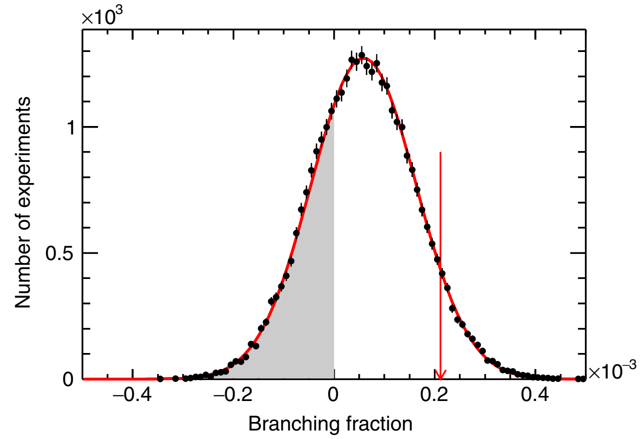

FIG. 3. Distribution of branching fractions determined from toy samples and a Gaussian fit, which are marked as dots with uncertainties and solid line, respectively. The shaded area represents the nonphysical region and the red arrow points to the position of upper limit at the 90% confidence level.

ACKNOWLEDGMENTS

The BESIII Collaboration thanks the staff of BEPCII and the IHEP computing center for their strong support. This work is supported in part by National Key Research and Development Program of China under Grants. No. 2020YFA0406400 and No. 2020YFA0406300; National Natural Science Foundation of China (NSFC) under Contracts No. 11625523, No. 11635010, No. 11735014, No. 11805086, No. 11822506, No. 11835012, No. 11935015, No. 11935016, No. 11935018, and No. 11961141012; the Chinese Academy of Sciences (CAS) Large-Scale Scientific Facility Program; the CAS PIFI program; Joint Large-Scale Scientific Facility Funds of the NSFC and CAS under Contracts No. U1732263 and No. U1832207; CAS Key Research Program of Frontier Sciences under Contracts No. QYZDJ-SSW-SLH003 and No. QYZDJ-SSW-SLH040; 100 Talents Program of CAS; the Fundamental Research Funds for the Central Universities; The Institute of Nuclear and Particle Physics (INPAC) and Shanghai Key Laboratory for Particle Physics and Cosmology; ERC under Contract No. 758462; European Union Horizon 2020 research and innovation programme under Contract No. Marie Sklodowska-Curie grant agreement No. 894790; German Research Foundation DFG under Contracts No. 443159800, Collaborative Research Center CRC 1044, Grant No. FOR 2359 and No. GRK 2149; Istituto Nazionale di Fisica Nucleare, Italy; Ministry of Development of Turkey under Contract No. DPT2006K-120470; National Science and Technology fund; Olle Engkvist Foundation under Contract No. 200-0605; STFC (United Kingdom); The Knut and Alice Wallenberg Foundation (Sweden) under Contract No. 2016.0157; The Royal Society, UK under Contracts No. DH140054 and No. DH160214; The Swedish Research Council; U.S. Department of Energy under Contracts No. DE-FG02-05ER41374 and No. DE-SC-0012069.

[1] S. L. Glashow, J. Iliopoulos, and L. Maiani, Phys. Rev. D **2**, 1285 (1970).
[2] D. M. Asner *et al.*, Int. J. Mod. Phys. A **24**, 499 (2009).
[3] M. Saur and F. S. Yu, Sci. Bull. **65**, 1428 (2020).
[4] G. Wilkinson, Sci. Bull. **66**, 2251 (2021).
[5] L. Cappiello, O. Cata, and G. D'Ambrosio, J. High Energy Phys. 04 (2013) 135.
[6] R. Aaij *et al.* (LHCb Collaboration), Phys. Rev. Lett. **119**, 181805 (2017).
[7] G. Burdman, E. Golowich, J. A. Hewett, and S. Pakvasa, Phys. Rev. D **66**, 014009 (2002).
[8] I. I. Bigi and A. Paul, J. High Energy Phys. 03 (2012) 021.
[9] A. Paul, I. I. Bigi, and S. Recksiegel, Phys. Rev. D **83**, 114006 (2011).
[10] R. Bause, H. Gisbert, M. Golz, and G. Hiller, Phys. Rev. D **103**, 015033 (2021).
[11] S. Fajfer and A. Novosel, Phys. Rev. D **104**, 015014 (2021).
[12] R. Aaij *et al.* (LHCb Collaboration), Nat. Phys. **18**, 277 (2022).
[13] R. K. Ellis *et al.*, arXiv:1910.11775.
[14] I. Doršner, S. Fajfer, A. Greljo, J. F. Kamenik, and N. Košnik, Phys. Rep. **641**, 1 (2016).
[15] G. Faisel, J. Y. Su, and J. Tandean, J. High Energy Phys. 04 (2021) 246.
[16] M. Ablikim *et al.* (BESIII Collaboration), Chin. Phys. C **37**, 123001 (2013); Phys. Lett. B **753**, 629 (2016).
[17] M. Ablikim *et al.* (BESIII Collaboration), Chin. Phys. C **42**, 083001 (2018).
[18] M. Ablikim *et al.* (BESIII Collaboration), Nucl. Instrum. Methods Phys. Res., Sect. A **614**, 345 (2010).
[19] M. Ablikim *et al.* (BESIII Collaboration), Phys. Rev. D **97**, 072015 (2018).
[20] M. Ablikim *et al.* (BESIII Collaboration), Phys. Rev. D **92**, 072012 (2015).
[21] R. M. Baltrusaitis *et al.* (MARK-III Collaboration), Phys. Rev. Lett. **56**, 2140 (1986); J. Adler *et al.* (MARK-III Collaboration), Phys. Rev. Lett. **60**, 89 (1988).
[22] H. B. Li and X. R. Lyu, Natl. Sci. Rev. **8**, nwab181 (2021).
[23] X. Zhou, S. Du, G. Li, and C. Shen, Comput. Phys. Commun. **258**, 107540 (2021).
[24] M. N. Achasov *et al.*, J. Instrum. **10**, P09006 (2015).
[25] M. Ablikim *et al.* (BESIII Collaboration), Chin. Phys. C **41**, 013001 (2017).
[26] A. Rogozhnikov, J. Phys. Conf. Ser. **762**, 012036 (2016).
[27] P. A. Zyla *et al.* (Particle Data Group), Prog. Theor. Exp. Phys. **2020**, 083C01 (2020).
[28] J. P. Lees *et al.* (*BABAR* Collaboration), Phys. Rev. D **85**, 091107 (2012).
[29] M. Ablikim *et al.* (BESIII Collaboration), Phys. Rev. D **91**, 112015 (2015); **95**, 071102 (2017).
[30] M. Ablikim *et al.* (BESIII Collaboration), Chin. Phys. C **44**, 040001 (2020).